Structural dynamics of dispersed titania during dehydration and oxidative dehydrogenation studied by *in situ* UV Raman spectroscopy

Philipp Waleska, Christian Hess*

Eduard-Zintl-Institut für Anorganische und Physikalische Chemie, Technische Universität Darmstadt, Alarich-Weiss-Str. 8, 64287 Darmstadt, Germany

*hess@pc.chemie.tu-darmstadt.de

Abstract

The structural dynamics of dispersed titania, i.e., silica supported titania, is investigated during dehydration and oxidative dehydrogenation (ODH) of ethanol using optical spectroscopy. UV Raman spectroscopy enabling resonance enhancements proves to be a valuable tool to identify Ti-OH, Ti-O-Si, and Ti-O-Ti groups. Upon dehydration, a transformation of Ti-OH into Ti-O-Si and Ti-O-Ti groups is observed. Two types of Ti-OH vibrations (isolated, geminal) are identified at around 700 and 800 cm^{-1} in agreement with theoretical models. Dispersed titania is catalytically active in ethanol ODH with a performance comparable to dispersed vanadia. *In situ* UV Raman spectra reveal a consumption of Ti-O-Ti, Ti-O-Si, and Ti-OH groups during ethanol adsorption to the titania surface. The presented results are consistent with an ODH reaction mechanism involving a structural transformation of oligomerized or closely neighbored monomeric TiO_X structures. The relevance of the proposed mechanism is discussed in the context of other supported transition metal oxides catalysts.

Keywords: titania, UV Raman spectroscopy, oxidative dehydrogenation (ODH), *in situ*, structural dynamics

1. Introduction

Crystalline as well as dispersed titania is known to be a promising material in the field of (photo)catalysis.[1-4] TiO_2-supported vanadia and supported titanium-vanadium oxide have been widely used as catalysts, e.g. in the selective catalytic reduction (SCR) of nitrogen oxides with ammonia or the oxidative dehydrogenation (ODH) of ethanol and propane.[5-13] According to the literature, the use of titania as a support material for dispersed vanadia as well as mixing dispersed titania to SiO_2-supported vanadia leads to a significant improvement of the catalytic activity in oxidation reactions.[5-6, 8, 12-15] Due to its redox properties titania has been considered an active support material. Gao et al. reported on the catalytic performance of SiO_2-supported titania during the ODH of methanol.[1] Moreover, Dinse et al. have shown titania to be directly involved in the ODH of propane over titania supported vanadia catalysts based on the increased amount of reduced titania (Ti^{3+}) observed in EPR spectra recorded after reaction.[15] To the best of our knowledge, there have been no previous reports on the ODH of ethanol over dispersed titania.

Previous spectroscopic and theoretical studies have demonstrated that dispersed titania is composed of monomeric and/or oligomeric TiO_X species depending on coverage.[1, 16-21] According to Gao et al. in SiO_2-supported titania at low loadings (0.24 Ti/nm^2) predominantly isolated TiO_4 species are present, whereas at higher loadings (~4 Ti/nm^2) two-dimensional oligomers of TiO_5 units dominate.[1] Besides, using vibrational spectroscopy on silica SBA-15 supported titania (0.7 Ti/nm^2) in combination with normal-mode analysis, Nitsche and Hess validated the presence of hydroxyl groups in dispersed titania.[16] Previous Raman studies on the structure of dispersed titania were limited almost exclusively on the interphase, i.e., Ti-O-Si bonds,[1, 17-21] while it would be highly desirable to find spectroscopic markers for Ti-O-Ti and Ti-OH bonds. Thus, based on the current state of knowledge it is probably fair to say, that a

detailed structural knowledge of molecularly dispersed titania is still missing despite its relevance for a detailed understanding of the role of titania in heterogeneous catalysis.

Thus, in an attempt to advance the level of structural analysis of dispersed titania, we applied resonance Raman spectroscopy by moving the laser excitation wavelength into the UV to allow for resonant excitation of titania electronic transitions. We show that, by such an approach, important aspects of the structural changes of the titania surface including the detection of adsorbed species were accessible under *in situ* conditions. Based on these new spectroscopic findings on the titania surface structure we propose a mechanism for the structural dynamics of dispersed titania during ODH of ethanol.

2. Experimental section

Sample preparation. The used sample consists of mesoporous silica (SBA-15) as support material and a defined amount of titania dispersed onto the surface of the support. The synthesis of SBA-15 was described previously in the literature.[22] Titania was deposited onto the silica support via incipient wetness impregnation using a precursor solution of titanium(IV) isopropoxide ($Ti(iOPr)_4$, Sigma Aldrich, 99.999 %) and 2-propanol (anhydrous, Sigma Aldrich) with a concentration c_{Ti} = 0.34 mol l^{-1}. For the impregnation, 1 g of SBA-15 was first dried overnight at 85 °C and then loaded in a drop-wise fashion with the precursor solution (1.5 ml) to yield a titania loading of 0.5 Ti nm^{-2}. After this step, the sample was calcined at 550 °C for 12 h (ramp rate: 1.5 °C min^{-1}). The specific surface area of the prepared sample was determined to be 612 m^2 g^1 by using the Brunauer-Emmet-Teller method (BET). In the following, this sample will be referred to as 0.5 TiO_X/SBA-15. TiO_2 anatase (Sigma Aldrich, 99.8 %) and AEROXIDE TiO_2 P 25 (Evonik, ≥99.5 wt%) were used as purchased.

Raman spectroscopy. UV Raman spectra were recorded with a spectrometer equipped with a titanium:sapphire (Ti:Sa) solid state laser (Indigo-S, Coherent), a triple-stage spectrograph

(Princeton Instruments, TriVista 555), and a charge-coupled device (CCD) camera with 2048 × 512 pixels (Princeton Instruments, Spec10:2kBUV). Frequency-tripling of the Ti:Sa emission is accomplished by anisotropic BBO (BaB_2O_4) and LBO (LiB_3O_5) crystals. A more detailed description of the spectrometer can be found elsewhere.[23-24] Specifications of the spectrometer are summarized in Table 1. The laser power used for the experiments was adjusted to 7-8 mW as measured at the position of the sample. To exclude laser damages caused by the UV excitation the radiation was softly focused (see Table 1) and continuously moved over the surface of the sample during the measurements.

Processing of the Raman spectra included a background subtraction, smoothing with a moving average filter, and an absorption correction based on the recorded UV-Vis spectra. Fitting analysis of Raman bands was performed using Voigt functions, which were calculated by a convolution of Gaussian and Lorentzian line profiles. As the half-width of the Gaussian function, the line broadening of the laser line was used. For spectral analysis Matlab R2010a and Origin 8.0 were employed.

Table 1. Specifications of the UV Raman spectrometer.

Laser wavelength (excitation source)	256.7 nm
Line broadening	10.8 cm^{-1}
Resolution	1 cm^{-1}
Spot size (focus)	0.6 mm^2

UV-Vis DR spectroscopy. UV-Vis spectra were recorded on a V770 UV-Vis/NIR spectrometer (JASCO) equipped with a halogen and a deuterium lamp, a photomultiplier, and a Peltier-cooled PbS detector. A praying mantis accessory (Harrick Scientific Products) was used to collect the diffuse reflected (DR) radiation. Spectra were recorded within 200-1000 nm with a wavelength accuracy of ±0.3 nm (Vis) and ±1.5 nm (NIR) using 0.5 nm steps. The bare SBA-15 support at room temperature was employed as white standard.

Catalytic testing. For catalytic tests 20 to 25 mg of the sample were filled into a CCR1000 reactor (Linkam Scientific Instruments). The samples were first dehydrated at about 300 °C for 1.5 h under oxidative conditions (8 vol.% O_2, 92 vol.% N_2) at a total gas flow of 50 ml min^{-1}. After dehydration, the gas-phase composition was switched to reaction conditions (1 vol.% ethanol, 8 vol.% O_2, and 91 vol.% N_2) and the temperature was increased gradually from 96 to 196 °C holding each step for at least 15 min. Ethanol (Sigma Aldrich, liquid, ≥99.8% (GC)) was mixed into the gas stream using a gas saturator cooled down to 8 °C. All gas lines from the gas saturator to the gas outlet were heated to 90 °C to avoid condensation of ethanol.

For gas-phase analysis, a Vertex 70 spectrometer (Bruker) equipped with a RT-DLaTGS detector was used. This Fourier-transform infrared (FTIR) spectrometer continuously monitored the gas stream exiting the reactor. A 25 ml sized gas cell (LFT 20520, Axiom Analytical Incorporated) heated to 125 °C was integrated in the FTIR spectrometer to record IR spectra of the gas phase with a collection time of 149.8 ± 0.2 s. The spectrometer resolution was 1 cm^{-1}, the aperture was set to 4 mm, and a spectral range from 1000 to 4000 cm^{-1} was selected.

To calculate the conversion and the selectivity, differences between the recorded FTIR spectra and spectra of reference substances were determined to isolate the characteristic signals of each product and reactant. Characteristic regions of the difference spectra were integrated via the trapezoidal method and the obtained areas were converted into concentrations using calibration

functions. Table 2 summarizes the chosen spectral regions used for the integration of the gas-phase compounds.

Table 2. IR spectral regions used for the integration of the gas-phase compounds.

Spectral region [cm^{-1}]	Gas
1679–1814	$H_3C–CH=O$
2058–2222	CO
2278–2392	CO_2
2885–2999	$H_3C–CH_2–OH$
3107–3252	$H_2C=CH_2$
3431–3985	H_2O

***In situ* spectroscopy.** *In situ* UV Raman experiments were performed using the CCR1000 reactor of Linkam Scientific Instruments, whereas the *in situ* UV-Vis experiments were carried out in a HVCMRA-5 cell by Harrick Scientific Products. Both cells were sealed with CaF_2 spectroscopic windows. The set temperature was continuously logged during the entire experiment.

To study the effect of dehydration, spectra were first recorded under ambient conditions in air at 26 °C followed by a dehydration step at 300 °C for 1.5 h. Spectra of the dehydrated sample were recorded again at 26 °C in synthetic air (UV-Vis: 20 vol.% O_2, 80 vol.% N_2; Raman: 8 vol.% O_2, 92 vol.% N_2). The sample was then heated to 128 °C to investigate the effect of temperature on the spectroscopic data.

The spectroscopic investigation of the ODH of ethanol was carried out in three different steps. At first, the sample was dehydrated under oxidative conditions (and 8 vol.% O_2, 92 vol.% N_2).

Temperature and duration of the dehydration step were chosen as described above. After dehydration, the temperature was set to 128 °C and held constant for the remainder of the experiment. Next, a spectrum prior to the reaction was recorded at a reaction temperature of 128 °C under oxidative conditions. The gas-phase composition was then switched to reaction conditions (1 vol.% ethanol, 8 vol.% O_2 and 91 vol.% N_2) and spectra were taken after equilibration of the reaction (10 min).

3. Results

Catalytic activity. Figure 1 shows the conversion and the selectivity of SiO_2-supported titania with a loading of 0.5 Ti/nm^2 (0.5 TiO_X/SBA-15) in the ODH of ethanol in comparison to the bare silica support. Starting at a temperature of 128 °C the difference in conversion of dispersed titania and the bare support increases significantly clearly indicating additional catalytic activity of dispersed titania. At higher temperatures the catalytic activity of dispersed titania increasingly dominates over that of the support material. The temperature of 128 °C was chosen as the reaction temperature for the *in situ* experiments discussed below. Please note that at 128 °C the conversion of dispersed titania is 0.97 ± 0.03 % corresponding to about half the conversion of dispersed vanadia under the same loading (0.5 V/nm^2 on silica SBA-15, 0.5 VO_X/SBA-15) and reaction conditions.[25] The selectivity towards acetaldehyde at this temperature is 97.6 ± 0.2% with CO_2 as the only detected byproduct. With increasing temperature and conversion the selectivity towards acetaldehyde decreases for dispersed titania as well as for the bare support. At 196 °C, small amounts of CO are observed in the gas-phase for dispersed titania besides CO_2.

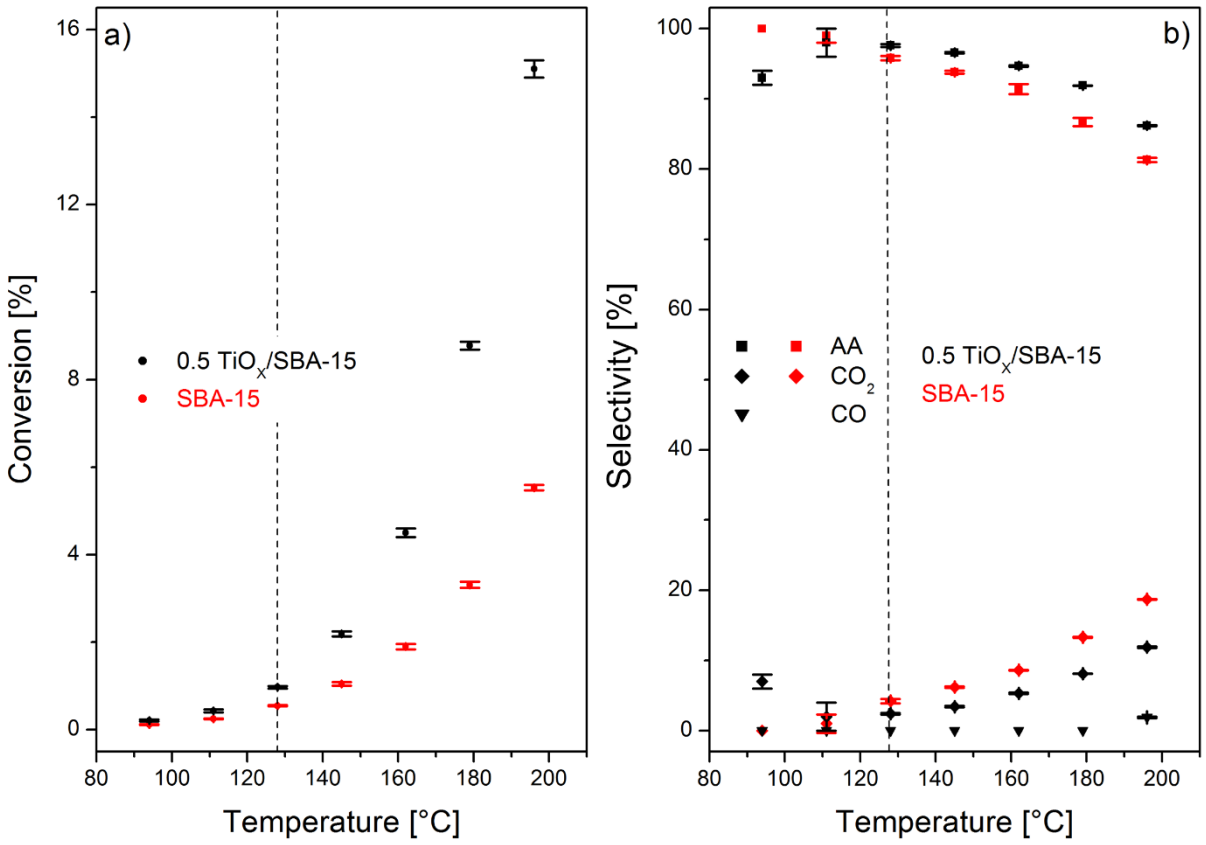

Figure 1. Conversion (left) and selectivity (right) during ODH of ethanol as a function of temperature for SiO_2-supported titania with a loading density of 0.5 Ti/nm^2 (0.5 TiO_X/SBA-15) (black) compared to the bare silica SBA-15 support (red). Gas composition: 1 vol.% ethanol, 8 vol.% O_2, 91 vol.% N; total flow rate: 50 ml min^{-1}. The temperature, at which *in situ* experiments were performed, is marked with a dashed line.

***In situ* characterization.** Figure 2 depicts Raman and UV-Vis spectra of 0.5 TiO_X/SBA-15 as well as two crystalline titania powder samples used as references. The first reference contains only the anatase phase of TiO_2, while the second (P-25) contains a mixture of rutile and anatase in a 3:1 ratio.[26] The three UV-Vis spectra are characterized by strong absorption in the UV range, whereas visible absorption for wavelengths > 400 nm is negligible. Consistent with the UV-Vis results all samples have a white color. As indicated in Figure 2, the wavelength of the laser used for the Raman spectroscopic experiments is located at 256.7 nm, i.e., within the

strong UV absorption band of the samples. Thus, during Raman spectroscopy electronic transitions are excited, which give rise to resonance enhancements. As a result of resonance effects, overtones bands are observed.

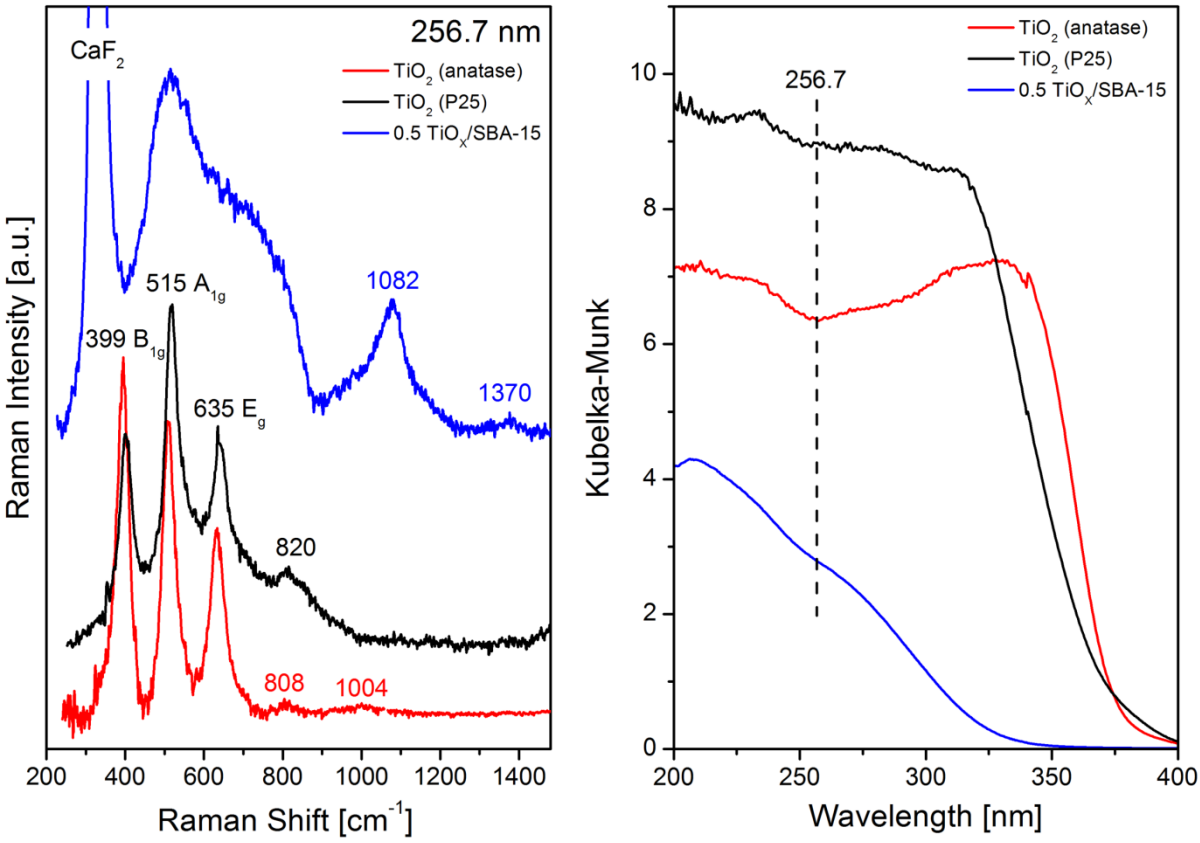

Figure 2. Left: Raman reference spectra (256.7 nm) of TiO_2, anatase (red) and TiO_2, P-25 (black) in comparison to 0.5 TiO_X/SBA-15 (blue) recorded at room temperature (26°C). All spectra were recorded under ambient conditions in air. Reference spectra were recorded without sealing the reaction chamber with a CaF_2 window. Right: Corresponding UV-Vis spectra. All spectra were measured under ambient conditions at 26 °C. The laser wavelength used for the Raman experiments (256.7 nm) is marked in the UV-Vis spectra. Raman spectra were corrected for absorption. Raman spectra of P-25 and 0.5 TiO_X/SBA-15 were offset for clarity.

In the Raman spectra of the two reference compounds, three sharp peaks are observed at 399, 515, and 636 cm^{-1}, which can be assigned to the main signals of the anatase phase, in agreement with the literature.[3, 27-29] The anatase phase of TiO_2 belongs to the space group D_{4h} with an elongated unit cell containing two TiO_2 units with lattice constants of a = 0.3783 and c = 0.951 nm. Thus, there are 15 vibrational modes in total, six of which are Raman allowed.[28, 30] Two anatase signals are located at 144 and 197 cm^{-1}, but could not be observed in the presented Raman spectra recorded at > 200 cm^{-1}. In accordance with the literature, a fitting analysis of the two reference spectra reveals a superposition of two Raman bands at 515 cm^{-1}, one of which is totally symmetric (A_{1g}).[3, 28] Therefore, we attribute the small feature at 1004 cm^{-1} in the spectrum of pure anatase TiO_2 to the first overtone of this A_{1g} mode. The additional anatase feature located at 808 cm^{-1} is assigned to a combination band.[28] In the literature, the anatase features within the range 400-700 cm^{-1} have been assigned to either O-Ti-O deformation or Ti-O stretching vibrations of the TiO_2 network.[3, 28] The broad band at 820 cm^{-1} observed for P-25 is a characteristic feature of the rutile phase.[27, 31] The rutile phase of TiO_2 also belongs to the space group D_{4h} and has four allowed Raman modes.[31] Besides the feature at 820 cm^{-1} the other three rutile signals could not be observed in the spectrum of P-25, but may contribute to the high underground signal within the range 200-1000 cm^{-1}. It is noteworthy, that the characteristic anatase signals of P-25 have a different intensity ratio as compared to bare anatase, which may be explained by different ratios of titania (101) to (001) surfaces in the two samples.[3]

As shown in Figure 2, the spectrum of dispersed titania (0.5 TiO_X/SBA-15) reveals two broad and structured Raman bands located within 200-900 cm^{-1} and 900-1200 cm^{1}, respectively. Besides, a small band at 1370 cm^{-1} is observed. The sharp and intensive peak at 325 cm^{-1} originates from the CaF_2 window of the reaction cell. The band at around 1082 cm^{-1} has been well studied in the literature and is characteristic for dispersed TiO_X species.[16, 19]

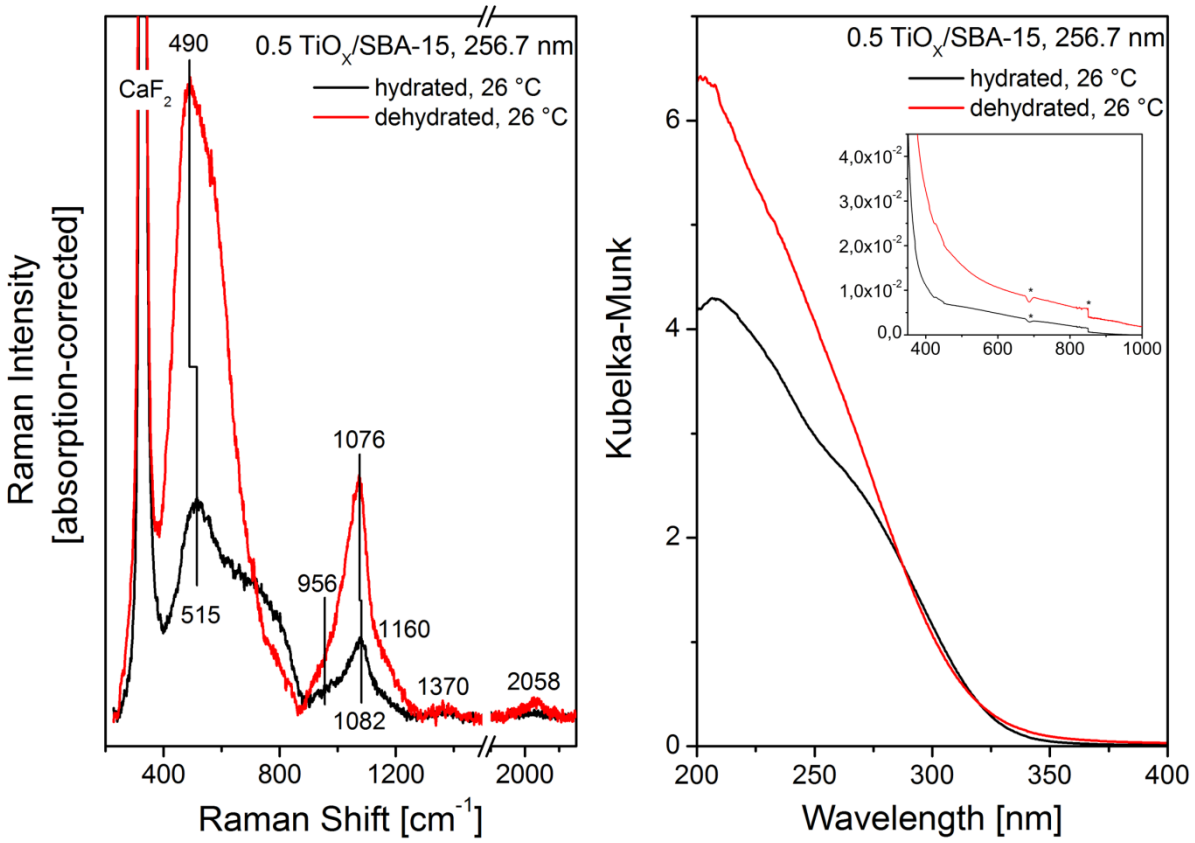

Figure 3. Left: Raman spectra (256.7 nm) of 0.5 TiO_X/SBA-15 in its hydrated (black) and dehydrated (red) state recorded at 26 °C. Right: Corresponding UV-Vis spectra. The inset gives an enlarged view of the Vis/NIR region. Spectra of hydrated samples were recorded under ambient conditions in air. For dehydration samples were treated in synthetic air (total gas flow: 50 ml min^{-1}) at 300 °C for about 90 min and then cooled down in synthetic air to room temperature to record spectra (UV-Vis: 20 vol.% O_2, 80 vol.% N_2; Raman: 8 vol.% O_2, 92 vol.% N_2).

Dehydration of sample 0.5 TiO_X/SBA-15 results in a dramatic change of the spectral profiles of the two main Raman bands (see Figure 3, left panel). The intensity of both bands increases significantly, while the maxima show redshifts from 515 to 490 cm^{-1} and from 1082 to 1076 cm^{1}, respectively. Upon dehydration, an additional feature at around 2060 cm^{-1} appears.

Beside the main signal at 1076 cm^{-1}, two additional features at 956 and 1160 cm^{-1} as well as a small shoulder at around 1030 cm^{-1} can be identified in the spectrum of the dehydrated sample as a result of the increased intensity within 900-1200 cm^{-1}. Based on theoretical considerations, the two features at 956 and 1030 cm^{-1} are assigned to interphase vibrations, whereas the feature at 1076 cm^{-1} is attributed to in phase / out of phase Ti-O-Si stretching vibrations.[16] The shoulder at 1160 cm^{-1} is assigned titanium-containing silica, i.e., titanium incorporated into the silica SBA-15 matrix during preparation, besides LO/TO phonons from the silica support as discussed previously.[17] The band at 2058 cm^{-1} is assigned to the first overtone of the interphase band at 1030 cm^{-1} as will be discussed below. Please note that, while the overall intensity strongly increases during dehydration, the hydrated sample exhibits a higher intensity within 700-850 cm^{-1}.

As shown in the right panel of Figure 3, dehydration leads to an overall increase of the UV-Vis absorption of 0.5 TiO_X/SBA-15. In the UV-Vis spectra three absorption bands at around 210, 230, and 280 nm as well as a broad absorption in the Vis/NIR region can be identified. The absorption maximum of the hydrated sample at 200 nm is slightly redshifted with respect to the maximum of the dehydrated sample at 210 nm, while the feature at 280 nm is slightly more broadened in the UV-Vis spectrum of the hydrated sample as compared to that of the dehydrated sample. In the literature, absorption bands at around 210, 230, and 280 nm have been associated with charge transfer between an oxygen ligand, i.e., -O-Si, -O-H or –O-Ti, and the Ti^{4+} metal center.[1, 16, 17, 32-34] The two bands at 210 and 230 nm were assigned to isolated, tetrahedrally coordinated TiO_4 species. Klein et al. associated the absorption band at 280 nm with a higher coordinated TiO_X species, while Gao et al. as well as Nitsche and Hess assigned this band to oligomerized TiO_5.[1, 17, 32] Furthermore, Klokishner et al. verified theoretically that the absorption band of dispersed titania is a superposition of absorptions associated with different TiO_X species, where the absorption bands of oligomeric structures are redshifted in comparison

to those of monomeric structures.[34] Klokishner et al. also associated absorption bands at $\lambda > 400$ nm to the presence of reduced Ti^{3+} centers.[34] Based on a study on titania anatase single crystals, Sekiya et al. were able to assign several absorption band in the Vis/NIR region to d-d transitions indicating the presence of oxygen vacancies.[35]

Figure 4 depicts Raman spectra (256.7 nm) of 0.5 TiO_X/SBA-15 during oxidative and reaction conditions at 128 °C. Upon exposure to ethanol ODH conditions, distinct changes of the spectrum are observed. The Raman bands related to the dispersed TiO_X species are significantly decreased as compared to the spectrum prior to reaction. Besides, a series of new bands appears at 640, 930, 1071, 1133, and 1361 cm^1. Based on a Raman study of chlorinated and nonchlorinated titanium ethoxide, these features can be attributed to ethoxy coupled to TiO_X species.[36] In detail, the first four Raman bands were assigned to Ti-O stretching, C-C stretching, C-O stretching, and CH_3 rocking, respectively, whereas the bands at 1361 cm^{-1} was associated with a CH_3 deformation mode. The large linewidth of the CH_3 rocking band at 1133 cm^{-1} is consistent with the presence of two closely located features assigned to an in plane and an out of plane CH_3 motion according to Finnie et al.[36] Furthermore, the study on polychlorinated titanium alkoxides shows that bridged ethoxy species exhibit Raman bands at around 900 and 1090 cm^{-1}.[36] Since no Raman bands can be observed at these positions in the spectra of TiO_X/SBA-15, the adsorbed ethoxy species must be terminally coordinated. Moran et al. observed increased intensities for the C-C, C-O, and CH_3 Raman bands of titanium tetraisopropoxide under pre-resonance conditions concluding that these modes possess an additional vibrational component of the TiO_4 oscillator.[37] It is obvious to assume the presence of a similar group vibration for the resonance-enhanced Raman signals in this work. A fitting analysis in the range 900-1200 cm^{-1} reveals an additional shoulder at around 1030 cm^{-1}, which is assigned to one of the two interphase vibrations as discussed above, while the second is covered by stronger ethoxy-related feature at around 930 cm^{-1}.

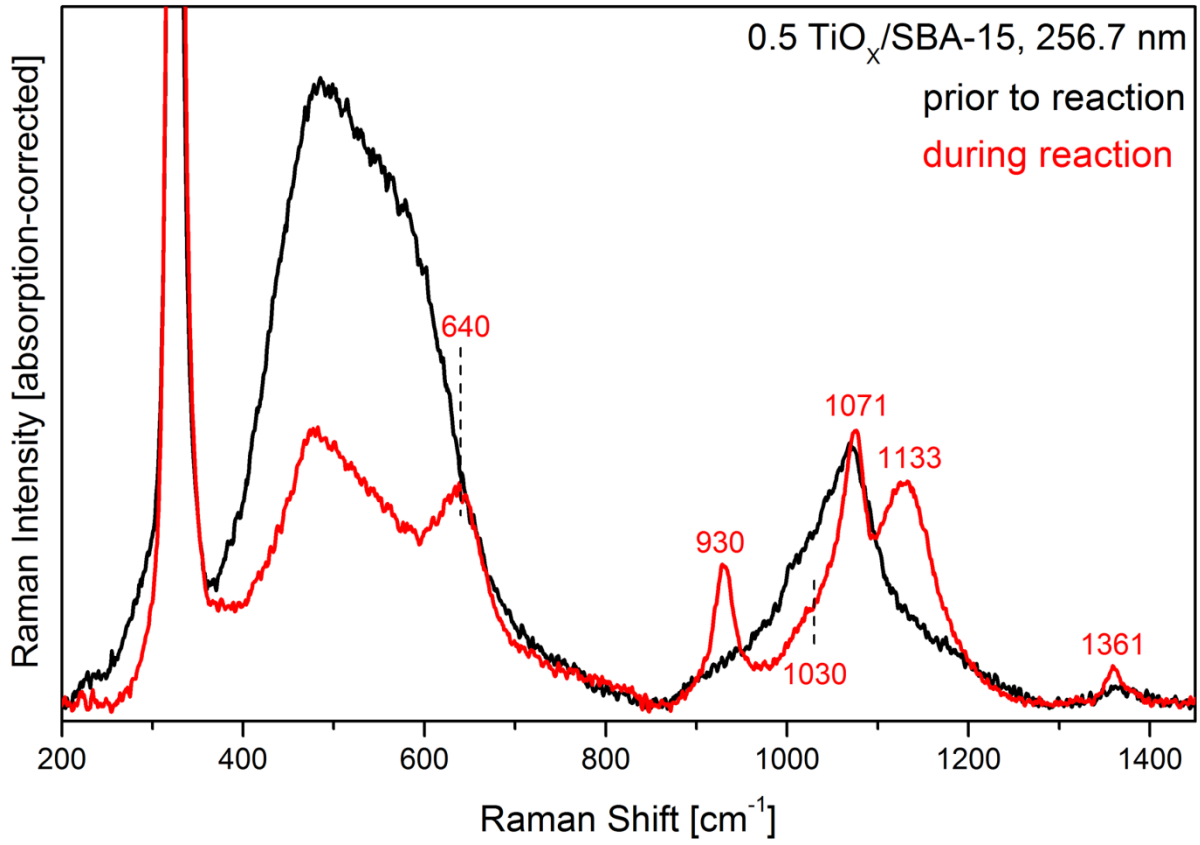

Figure 4. Raman spectra (256.7 nm) of 0.5 TiO_X/SBA-15 prior to (black) and during (red) ODH of ethanol at 128°C showing the low-wavenumber region. Prior reaction: 8 vol.% O_2, 92 vol.% N_2; during reaction: 1 vol.% ethanol, 8 vol.% O_2, 91 vol.% N_2; total flow rate: 50 ml min^{-1}. All spectra were corrected for absorption.

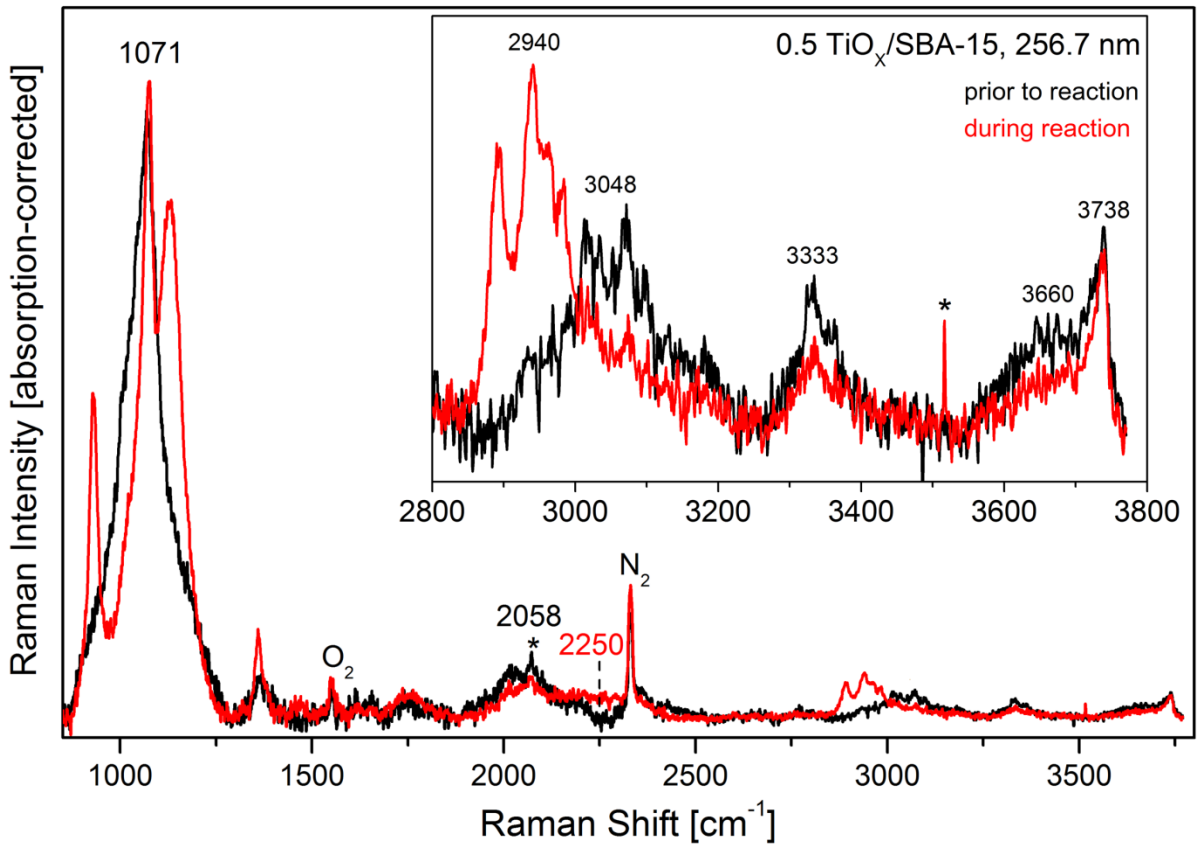

Figure 5. Raman spectra (256.7 nm) of 0.5 TiO_X/SBA-15 prior to (black) and during (red) ODH of ethanol at 128°C showing the high-wavenumber region. Prior reaction: 8 vol.% O_2, 92 vol.% N_2; during reaction: 1 vol.% ethanol, 8 vol.% O_2, 91 vol.% N_2; total flow rate: 50 ml min^{-1}. The inset gives an enlarged view on the C-H and the hydroxyl stretching region of the spectra. All spectra were corrected for absorption. The marked (*) sharp features result from cosmic rays.

Figure 5 gives an extended view on the Raman spectra (256.7 nm) of 0.5 TiO_X/SBA-15 during oxidative and reaction conditions. The sharp features at 1552 and 2331 cm^{-1} originate from gas-phase oxygen and nitrogen, respectively.[24] Broad features observed at around 2060 and 3050 cm^{-1} are associated with the first and second overtone of the of the interphase band at 1030 cm^{-1}, respectively. Upon exposure to reaction conditions, their intensities decrease. Under reaction conditions, several new Raman features are identified within 2000-3000 cm^{-1}. The band at around 2250 cm^{-1} is assigned to a combination band of the C-O stretching and the CH_3 rocking

vibration at 1071 and 1133 cm^{-1}, respectively, whereas the quartet of four sharp peaks at around 2940 cm^{-1} (see inset of Figure 5) can be attributed to the C-H stretching vibrations of adsorbed ethoxy species, in agreement with the literature.[1, 37] In addition, at wavenumbers > 3000 cm^{-1}, intensity changes in the hydroxyl stretching vibrations are observed upon switching to reactive conditions. A fitting analysis in the range 3600-3800 cm^{-1} reveals that the intensity of the sharp feature at 3738 cm^{-1} slightly decreases, while the broad band at around 3660 cm^{-1} is approximately halved in its intensity. The Raman feature at 3738 cm^{-1} originates from isolated silanol groups of the SBA-15 support.[25] Previously, based on IR experiments on dispersed titania, Nitsche and Hess assigned the feature at 3660 cm^{-1} to a Ti-OH stretching vibration.[17] At last, another broad Raman feature at 3333 cm^{-1} can be observed, which shows a decrease in intensity under reaction conditions (see inset of Figure 5). This feature was also present in Raman experiments on bare SBA-15 exhibiting a small intensity decrease upon dehydration. The observed behavior is consistent with hydroxyl stretching of hydrogen bonded silanol groups or residual water molecules bound within smaller channels (e.g. micropores) of the mesoporous silica matrix partly reduced due to ethanol adsorption to the surface. [38]

Discussion

Structure of dispersed titania. The UV Raman spectrum of dispersed titania shows a broad and intense band within 400-950 cm^{-1} (see Figure 2), which is composed of several contributions. Since we were able to identify five main signals during the analysis of the two titania reference compounds in Figure 2, we performed a detailed fitting analysis of this band using Voigt functions yielding Raman bands at around 460, 515, 630, 745, und 825 cm^{-1}. In contrast to the sharp peaks of the two crystalline titania references, all fitted bands are strongly broadened due to a disordered, amorphous-like structure. Nevertheless, some of the fitted band positions match quite well with those of crystalline signals representative of Ti-O stretching

vibrations. Hardcastle et al. studied the structure of amorphous titania using Raman spectroscopy at laser wavelengths of 514.5 and 632 nm and identified three signals at 450, 580, and 680 cm^{-1}, which were assigned to Ti-O stretching vibrations.[27] Vuurman and Wachs studied Al_2O_3-supported titania identifying two features at 460 and 710 cm^{-1}, which they assigned to Ti-O-Ti vibrations.[39] Strunk et al. proposed the formation of oligomerized TiO_X species on a SiO_2-support, but an identification of characteristic Ti-O-Ti features using Raman spectroscopy (at 532 nm excitation) was difficult due to strong silica bands within 400-900 cm^{-1}.[21] Alternatively, Li and his co-workers associated Raman bands in the range 490-530 cm^{-1} with Ti-O-Si stretching and bending vibrations during UV Raman studies of SiO_2-supported titania.[18-19, 40] At last, Finnie et al. and Moran et al. studied the Raman spectra of various titanium alkoxides and observed several bands within 500 to 650 cm^{-1}, which were assigned to Ti-O stretching vibrations.[36-37] On the basis of this literature survey as well as the comparison with the Raman spectra of crystalline references, we propose to attribute the Raman bands from 400 to 750 cm^{-1} in the spectrum of dispersed titania to Ti-O stretching vibrations. The second coordination partner of the oxygen may be another titanium atom forming a Ti-O-Ti bridge or a silicon atom of a Ti-O-Si bond.

Effect of dehydration. In the following, the *in situ* Raman and UV-Vis spectra will be discussed to evaluate the structural changes associated with the dehydration of dispersed titania. The UV-Vis data in Figure 3 show an overall increase in absorption in the UV and Vis/NIR region upon dehydration. Sekiya et al. reported that during heating of titania under oxidative or inert atmosphere hydroxyl group are removed as water from the TiO_2 network leading to the formation of oxygen vacancies.[35] As a consequence, an increased Vis/NIR absorption was detected, which may also explain the behavior in the Vis/NIR region observed for dehydrated titania. Furthermore, Klein et al. suggested absorption changes in the UV region of titania-silica mixed oxides to be associated with a conversion of tetrahedral TiO_X species into octahedral

structures upon hydration.[32] Sample dehydration is expected to lead to the reverse transformation. While for dehydration of dispersed titania a distinct intensity increase in the absorption bands at around 210 and 230 nm is observed, the absorption band at 280 nm is slightly narrowed. Thus the observed behavior in the UV region may be explained by a change in coordination number upon water removal. A detachment of TiO_X species converting oligomerized structures into smaller fractions as observed for dispersed vanadia can be excluded as for such a scenario a decrease in absorption at 280 nm would have been expected.[25]

Based on results from theoretical modeling Nitsche and Hess proposed the region 810-880 cm^{-1} to be associated with Ti-OH stretching vibrations.[16] However, so far there has been no experimental confirmation of this hypothesis. Since a larger number of hydroxyl groups is expected in the hydrated state and the observed Raman intensity within 700-850 cm^{-1} decreases upon dehydration, it stands to reason to assign this spectral region to Ti-OH groups. Considering also the increased intensity at around 490 and 1076 cm^{-1}, we conclude that Ti-OH groups are converted into Ti-O-Si or Ti-O-Ti bonds upon dehydration. In this context, the redshifts of the two main maxima from 515 to 490 cm^{-1} and from 1082 to 1076 cm^{-1} shown in Figure 3 may be explained by changes of the group vibrations replacing -OH by -O-Ti or -O-Si ligands.

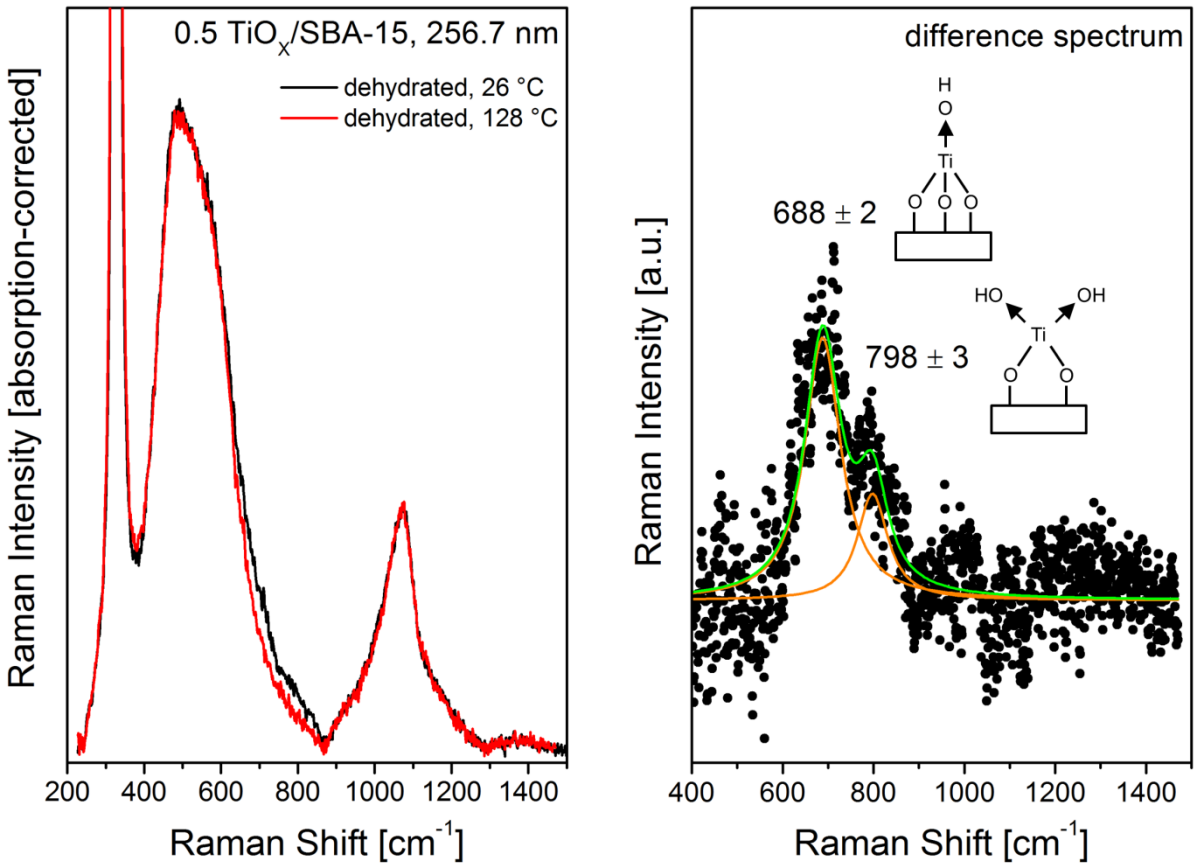

Figure 6. Left: Raman spectra (256.7 nm) of 0.5 TiO_X/SBA-15 at 26 °C (black) and 128 °C (red). Both spectra were recorded under oxidative conditions (8 vol.% O_2, 92 vol.% N_2) at a total gas flow of 50 ml min^1. The spectra were corrected for absorptions. Right: Difference spectrum of the Raman spectra shown on the left together with the results of a peak fitting analysis using Voigt functions.

For a more detailed analysis of the hydroxyl vibrations, dispersed titania was heated to 128 °C to continue the dehydration process. Figure 6 depicts UV Raman spectra of dehydrated 0.5 TiO_X/SBA-15 at 26 °C (black) and 128 °C (red) thus resembling differently dehydrated states of the sample. The spectra look largely the same except the region of the Ti-OH vibrations exhibiting a reduced intensity at 128 °C. In the difference spectrum of the two Raman spectra, shown in the right panel of Figure 6, two weak signals can be identified, whose positions were

determined as 688 ± 2 and 798 ± 3 cm^{-1} by peak-fitting analysis. Previously, Nitsche and Hess studied two different models of monomeric TiO_X species, which can be distinguished by the number of bonds to the support.[16] The first model is characterized by three Ti-O-Si bonds and one hydroxyl group, the second by two Ti-O-Si and two hydroxyl groups, respectively. Using a force constant of 4.63 mdyn $Å^{-1}$ for the Ti-O bond the band positions of the Ti-OH vibrations were calculated as 806 and 873 cm^{-1}. However, based on the new experimental results in Figure 6 we can conclude that the Ti-O bond exhibits a weaker force constant of about 3.3 mdyn $Å^{1}$. Applying this force constant to the models, the positions of the hydroxyl vibrations in the Raman spectrum perfectly match with the experimental results not affecting the positions of the other vibrations. The hydroxyl mode of the monomeric, tri-anchored TiO_X species is a total symmetric vibration. Therefore, we propose the weak signal at 1370 cm^{-1} to be the first overtone of this vibration.

ODH of ethanol. Figure 1 shows that dispersed titania is catalytically active in ethanol ODH. In the following, we will discuss the structural changes associated with the exposure to reaction conditions as derived from the *in situ* UV Raman data as well as their implications for the reaction mechanism of ethanol ODH over dispersed titania. As shown in Figure 4, switching from oxidative to reaction conditions leads to a decreased intensity of the broad Raman band at around 500 cm^{-1} and the shoulder at 1030 cm^{-1} indicating the consumption of Ti-O-Ti bridges and Ti-O-Si linkages as a result of ethanol adsorption. The adsorption of ethanol as an ethoxy species, that is terminally coordinated to the TiO_X structure, is demonstrated by the presence of characteristic ethoxy features in the Raman spectrum recorded under working conditions. In the region below ~1200 cm^{-1} a more detailed analysis of fundamental Raman bands related to TiO_X species during reaction, e.g. Ti-OH signals at around 700 cm^{-1}, is difficult because many bands are covered by strong adsorbate signals within 600-1200 cm^{-1} (see Figure 4). However, UV resonance Raman spectroscopy allows overtones to be exploited beside other higher

wavenumber modes such as O-H vibrations. Thus the UV Raman spectra of dispersed titania were analyzed within the range 1200-3800 cm^{-1} prior to and during reaction (see Figure 5). In this range structural changes of dispersed titania related to Ti-O-Si (overtone bands at around 2060, 3050 cm^{-1}) and TiO-H (3660 cm^{-1}) as well as adsorbate-related vibrations due to ethoxy (combination band at 2250 cm^{-1}, quartet at around 2940 cm^{-1}) can be detected. Under reaction condition, the consumption of TiO-H and SiO-H is observed. Based on an *operando* Raman study on indium oxide, Sänze et al. suggested a mechanism for the adsorption of ethanol involving the consumption of a hydroxyl group under elimination of water.[41] A similar scenario was proposed by Jehng et al. for the adsorption of methanol on silica.[42]

Based on our spectroscopic findings we propose the following reaction mechanism for ethanol ODH over dispersed titania (see Scheme 1): Under reaction conditions, Ti-O-Ti, Ti-O-Si, and Ti-OH groups are consumed enabling the adsorption of ethanol onto the TiO_X structure. As a result of ethanol adsorption ethoxy species are formed by breaking either Ti-O-Si or Ti-O-Ti linkages as indicated in Scheme 1. Concomitantly, adsorption of ethanol proceeds via Ti-OH (and Si-OH) groups under water elimination. For the conversion of ethoxy into acetaldehyde, two electrons need to be exchanged between catalyst and substrate, which requires the participation of two Ti^{4+} centers, since a reduction to Ti^{2+} is highly improbable.[43] On the other hand, the presence of Ti^{3+} has been validated by EPR e.g. after propane ODH over titania supported vanadia catalysts.[15] Thus it stands to reason that oligomerized or closely neighbored monomeric TiO_X structures are responsible for the catalytic activity. As indicated in Scheme 1, the electron exchange between catalyst and substrate is proposed to proceed via a radical ethoxy

intermediate formed by initial Ti-OCH_2CH_3 bond breakage and followed by H-abstraction leading to acetaldehyde and water formation.

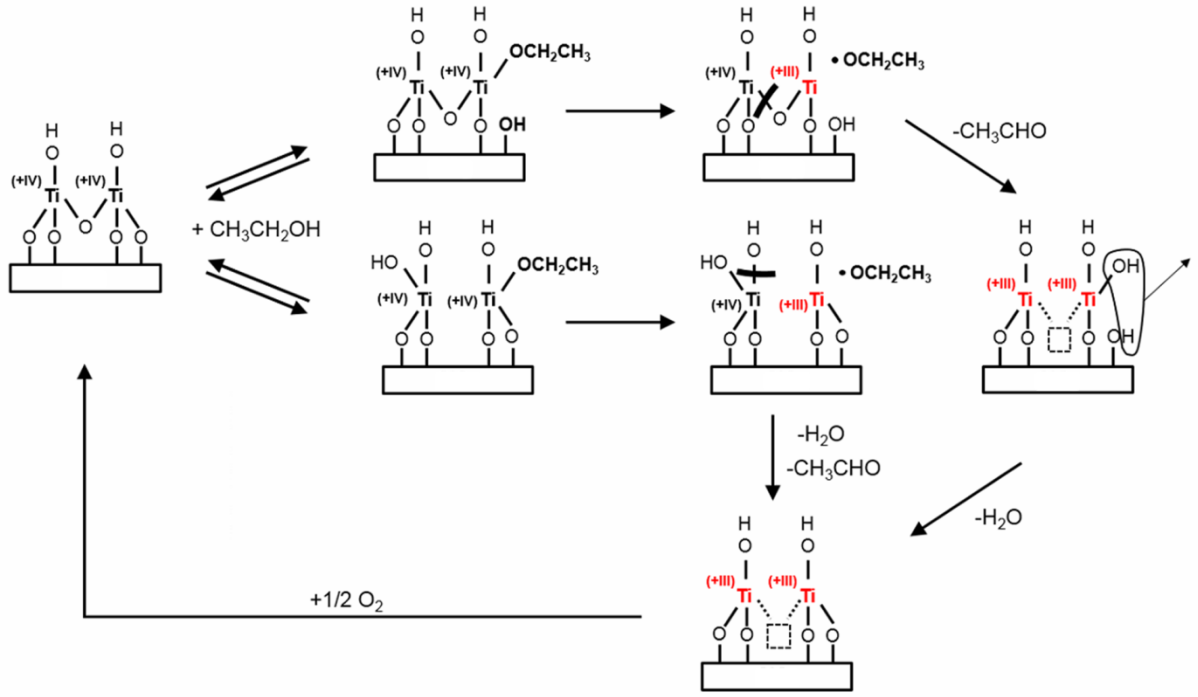

Scheme 1. Proposed reaction mechanism for the conversion of ethanol to acetaldehyde over dispersed titania.

It is worthwhile to discuss the mechanism outlined in Scheme 1 in the context of other transition metal oxide catalysts, in particular, dispersed vanadia catalysts. Recently, we studied the ODH of ethanol over silica SBA-15 supported vanadia catalysts with a loading of 0.5 V/nm^2 (0.5 VO_X/SBA-15) using directly comparable experimental conditions.[25] Interestingly, at 128 °C the conversion of dispersed titania amounts to about half the conversion of dispersed vanadia, while for both samples selectivities towards acetaldehyde are >96% and CO_2 is the only detected by-product. In contract to titania, dispersed surface vanadia species contain vanadyl (V=O) groups, which have been proposed to participate in the electron transfer between catalyst and substrate

based on experimental and theroretical findings.[25, 14] On the other hand, a reaction mechanism as outlined in Scheme 1 seems feasible also for dispersed vanadia catalysts. In such a scenario, the formation of radical ethoxides is accompanied by the reduction of two neighboring vanadium centers from V^{5+} to V^{4+} without the participation of vanadyl groups. Thus the above mechanism may be expected to play a more general role in the ODH of ethanol over transition metal oxide catalysts such as dispersed vanadia.

Conclusion

The structure of dispersed titania was studied and compared to well-known crystalline substances (anatase, rutile). Besides anatase- and rutile-derived features UV Raman spectra of dispersed titania revealed a broad band between 400 and 900 cm^{-1} due to Ti-O stretching vibrations as well as several overtones due to the resonance enhancement of the TiO_X structure. Upon dehydration, a redistribution and a significant increase of the intensity was observed indicating the transformation of Ti-OH into Ti-O-Si and Ti-O-Ti groups. Using UV Raman spectroscopy two types of TiO_X hydroxyl groups were accessible via Ti-OH stretching vibrations in the range 700-800 cm^{-1}. Based on previous theoretical calculations the two Raman bands at about 700 cm^{-1} and 800 cm^{-1} are assigned to terminal and germinal hydroxyl vibrations, respectively. In addition, dehydration of the sample leads to the formation of oxygen vacancies by removing hydroxyl groups from the structure of dispersed titania as indicated by a distinct increase of absorption in the Vis/NIR region.

Our results clearly demonstrate that dispersed titania is catalytically active in the ODH of ethanol. For the low conversions studied here selectivities towards acetaldehyde >95% were observed. It is remarkable that the conversion of dispersed titania corresponds to about half the conversion of dispersed vanadia under the same loading (0.5 M/nm^2 with M=V,Ti on silica SBA-15) and reaction conditions. *In situ* UV Raman spectra provides insight into the structural

changes upon exposure to the reaction conditions. To this end, adsorption of ethanol is accompanied by consumption of Ti-O-Ti, Ti-O-Si and Ti-OH groups enabling the formation of ethoxy species bound to the TiO_X structure. Considering operation of the redox couple Ti^{4+}/Ti^{3+} and the necessity of a two-electron exchange in ethanol ODH oligomerized or closely neighbored monomeric TiO_X structures are proposed to be responsible for the catalytic activity.

Acknowledgments

The authors would like to thank Severine Rupp and Patrick Ober for help with some of the Raman and UV-Vis experiments. Karl Kopp is acknowledged for technical support.

References

(1) Gao XT, Bare SR, Fierro JLG, Banares MA, Wachs IE (1998) J Phys Chem B 102:5653.

(2) Sannino D, Vaiano V, Ciambelli P, Carotenuto G, Di Serio M, Santacesaria E (2013) Catal Today 209:159.

(3) Tian F, Zhang YP, Zhang J, Pan CX (2012) J Phys Chem C 116:7515

(4) Dilla M, Schlögl R, Strunk J (2017) ChemCatChem 9:696

(5) Hamilton N, Wolfram T, Müller GT, Hävecker M, Kröhnert J, Carrero C, Schomäcker R, Trunschke A, Schlögl R (2012) Catal Sci Technol 2:1346

(6) Carrero C, Kauer M, Dinse A, Wolfram T, Hamilton N, Trunschke A, Schlögl R, Schomäcker R (2014) Catal Sci Technol 4:786

(7) Hess C, Waleska P, Ratzka M, Janssens TVW, Rasmussen SB, Beato P (2017) Top Catal 60:1631

(8) Andrushkevich TV, Kaichev VV, Chesalov YA, Saraev AA, Buktiyarov VI (2017) Catal Today 279:95

(9) Jørgensen B, Kristensen SB, Kunov-Kruse AJ, Fehrmann R, Christensen CH, Riisager A (2009) Top Catal 52:253

(10) Wachs IE, Deo G, Weckhuysen BM, Andreini A, Vuurman MA, deBoer M, Amiridis MD (1996) J Catal 161:211

(11) Segura Y, Chmielarz L, Kustrowski P, Cool P, Dziembaj R, Vansant EF (2005) Appl Catal B Environ 61:69

(12) Kwak JH, Herrera JE, Hu JZ, Wang Y, Peden CHF (2006) Appl Catal A 300:109

(13) Quaranta NE, Soria J, Corberán VC, Fierro JLG (1997) J Catal 171:1

(14) Beck B et al. (2012) J Catal 296:120

(15) Dinse A, Ozarowski A, Hess C, Schomäcker R, Dinse KP (2008) J Phys Chem C 112:17664

(16) Nitsche D, Hess C (2014) Chem Phys Lett 616:115

(17) Nitsche D, Hess C (2016) J Phys Chem C 120:1025

(18) Yang QH, Wang SL, Lu JQ, Xiong G, Feng ZC, Xin Q, Li C (2000) Appl Catal A 194:507

(19) Zhang L, Abbenhuis HCL, Gerritsen G, Ni Bhriain N, Magusin PCMM, Mezari B, Han W, van Santen RA, Yang QH, Li C (2007) Chem Eur J 13:1210

(20) Zhang WH, Lu JQ, Han B, Li MJ, Xiu JH, Ying PL, Li C (2002) Chem Mater 14:3413

(21) Strunk J, Vining WC, Bell AT (2010) J Phys Chem C 114:16937

(22) Ruff P, Lauterbach S, Kleebe HJ, Hess C (2016) Microp Mesop Mater 235:160

(23) Nitsche D, Hess C (2013) J Raman Spectrosc 44:1733

(24) Waleska PS, Hess C (2016) J Phys Chem C 120:18510

(25) Waleska PS, Rupp S, Hess C (2018) J Phys Chem C 122:3386

(26) Ohno T, Sarukawa K, Tokieda K, Matsumura M (2001) J Catal 203:82

(27) Hardcastle FD, Ishihara H, Sharma R, Biris AS (2011) J Mater Chem 21:6337

(28) Ohsaka T, Izumi F, Fujiki Y (1978) J Raman Spectrosc 7:321

(29) Zhang J, Xu Q, Li MJ, Feng ZC, Li C (2009) J Phys Chem C 113:1698

(30) Balachandran U, Eror NG (1982) J Solid State Chem 42:276

(31) Porto SPS, Fleury PA, Damen TC (1967) Phys Rev 154:522

(32) Klein S, Weckhuysen BM, Martens JA, Maier WF, Jacobs PA (1996) J Catal 163:489

(33) On DT, LeNoc L, Bonneviot, L (1996) Chem Commun:299

(34) Klokishner S, Reu O, Tzolova-Müller G, Schlögl R, Trunschke A (2014) J Phys Chem C 118:14677

(35) Sekiya T, Yagisawa T, Kamiya N, Das Mulmi D, Kurita S, Murakami Y, Kodaira T (2004) J Phys Soc Jpn 73:703

(36) Finnie KS, Luca V, Moran PD, Bartlett JR, Woolfrey JL (2000) J Mater Chem 10:409

(37) Moran PD, Bowmaker GA, Cooney RP, Finnie KS, Bartlett JR, Woolfrey JL (1998) Inorg Chem 37:2741

(38) Björklund S, Kocherbitov V (2017) Sci Rep 7:9960

(39) Vuurman MA, Wachs IE (1992) J Phys Chem 96:5008

(40) Li C (2003) J Catal 216:203

(41) Sänze S, Gurlo A, Hess C (2013) Angew Chem Int Ed 52:3607

(42) Jehng JM, Hu HC, Gao XT, Wachs IE (1996) Catal Today 28:335

(43) C.E. Housecroft, A.G. Sharpe Inorganic Chemistry (Pearson, Harlow, 2012)

Graphical abstract